

A THREE DIMENSIONAL COMBINED ELASTOPLASTIC AND DAMAGE MODEL FOR WOOD UNDER CYCLIC LOADING

Mingqian Wang

Ph.D. candidate, Tongji University, China
lwangmingqian@tongji.edu.cn

Xiaobin SONG

Associate professor, Tongji University, China
xiaobins@tongji.edu.cn

Xianglin Gu

Professor, Tongji University, China
gxl@tongji.edu.cn

Keywords: Wood; Combined elastoplastic and damage model; Plastic effects; Damage evolution; Cyclic loading

1 Objectives

Natural and engineered wood products are commonly used as load-bearing members in timber construction industry due to their physical and mechanical benefits, such as unique aesthetic values, high strength and stiffness to weight ratios, and outstanding energy dissipation capacity. Despite these attractive advantages, wood products are susceptible to damages induced by seismic loadings. Therefore, a better insight of the degradation process of the mechanical properties of wood, including stiffness degradation, strength softening behavior and irreversible deformation, is pertinent to numerical simulation of wood connections and members under cyclic loadings.

In general, analytical models can be only used in particular cases with rather rigid assumptions due to the anisotropic nature of wood. Finite element (FE) simulation work, as an alternative to analytic formulations, has gained increasing popularity for their ability of dealing with many practical 3-dimensional (3D) problems. However, one of the main challenging tasks of FE simulations is to consider complex mechanical behavior of wood, including ductile behavior and residential deformation under compression and brittle behavior under tension and/or shear.

Recently, the combined elastoplastic damage theory has been successfully adopted to predict the mechanical behavior of concrete and composite materials. Both the ductile and brittle failures can be accounted, and the irreversible deformation and softening behavior are explained via the classical

plastic theory and the continuum damage mechanics, respectively.

This study has therefore been aimed at extending the elastoplastic damage models to wood materials by choosing appropriate damage and softening laws. Strain increment based algorithm was developed and implemented in a commercial FE package, ABAQUS, with specific mesh and regularization techniques for stable convergence. The model was tested and validated based on test data in literature. Good results were obtained.

2 Model validation and discussion

2.1 Residential deformation

Cyclic loading tests of wood under longitudinal compression were conducted to inspect the model performance regarding the plastic (residual) deformation, strength softening behavior and stiffness degradation of wood members.

The specimens were prepared in conformance with the Standard test methods for small clear specimens of timber, ASTM D143-14 for secondary method specimens, i.e., 25×25 mm in cross-section and 100 mm in height. The measured moisture content of lumber was 9~13%. The displacement-controlled loading scheme was adopted with its loading rate of 0.1 mm/min. Fig. 1 illustrates the test setup of wood member under cyclic longitudinal compression.

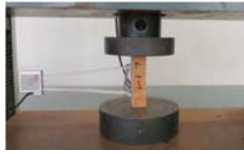


Fig.1 Test setup of wood under cyclic loading

For simplicity and to avoid localized damage, only one element, 8-node and fully integrated solid element, was used for model validation. The modulus of elasticity and the yielding compression strength were directly determined from the test results. The threshold strength for softening was determined by peak load. The hardening parameters were determined by fitting the nonlinear hardening branch, while the softening parameters were determined by fitting the softening branch. The other material properties were determined by the Wood Handbook. In addition to the elastic-plastic damage model proposed in this study, the elastic damage model was also tried and the results, as illustrated in Fig.2, were compared.

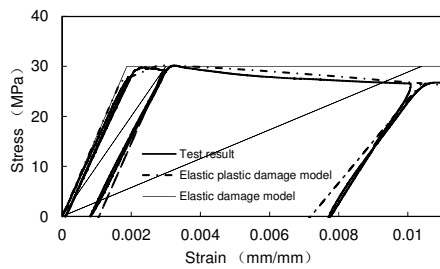


Fig.2 Stress-strain curves of wood with unloading

It is clear from Fig.2 that the model with elastic damage cannot describe the irreversible deformation at unloading since the calculation of Cauchy stresses in the elastic damage model does not consider the plastic strain. The elastic plastic damage model can accurately consider the residual deformation and stiffness degradation of wood under longitudinal compression.

2.2 Rotational behavior of traditional Chinese mortise and tenon connection

Numerical simulation of rotational behavior of traditional Chinese mortise and tenon connection was also carried out, since damage evolution of wood plays an important role in the strength softening behavior and stiffness degradation of such connections. FEM model of mortise and tenon connection is shown in Fig.3.

The moment-rotational angle curves of mortise and tenon connections are shown in Fig.4. It was found that the elastoplastic damage model could accurately

describe the strength softening behavior and stiffness degradation of such connections. The elastoplastic model may lead to an overestimation of stiffness and moment resistance of mortise and tenon connection at large displacement, since such model did not consider the damage evolution of wood.

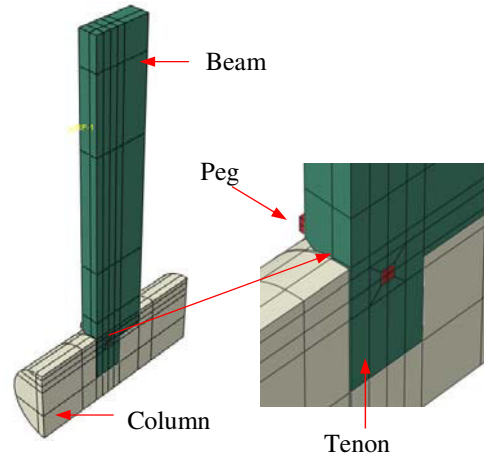


Fig.3 FEM model of mortise and tenon connection

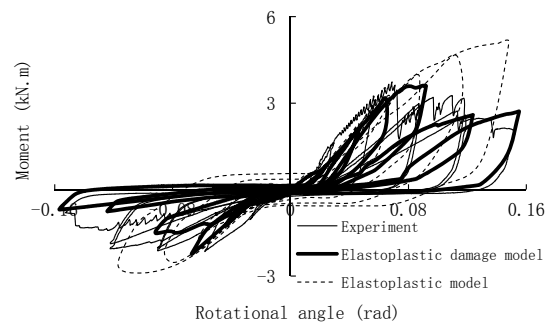


Fig.4 Moment-rotational angle curves of mortise and tenon connection

3 Conclusions

A combined elastic-plastic damage model was developed for the nonlinear analysis of wood under cyclic loadings. The plastic theory and continuum damage mechanics were applied to consider the ductile failure of wood in compression and brittle failure of wood in tension or shear. The constitutive model was implemented into a commercial FE software and validated with previous experimental and numerical studies. It was found that the proposed model could accurately trace the strength softening behavior, stiffness degradation and residual deformation of wood member and mortise and tenon connection.

POROSITY AND MECHANICAL PROPERTIES OF STEEL FOAMS PREPARED BY SPACE HOLDER TECHNIQUE

Huimeng WANG

Student, School of Civil Engineering, Xi'an University of Architecture and Technology, China
wanghuimeng029@163.com

Mingzhou SU

Professor, School of Civil Engineering, Xi'an University of Architecture and Technology, China
sumingzhou@163.com

Keywords: Steel foams; Space holder technique; Porosity; Mechanical properties

Porous metals possess a unique combination of properties, such as low density, low thermal conductivity and high energy absorption capacity. For structural applications, steel foams are much superior to aluminum foams due to their lower cost, higher strength and better weldability. Structure of steel foams can be characterized in terms of porosity, the shape and size distribution of pores, and defects in the pore wall structures. Among them, the porosity is regarded as the most important feature. However, how to predict the final porosity has been a challenge for this technique, because it is always not equal to the spacer content. Hence, the relationship between porosity (P) and spacer content (ϕ_1) was studied based on theory and practice in this paper. In addition, power law relations between mechanical properties and total porosity were frequently proposed to best fit experimental data in literatures. However, the physical significance of using the value of total porosity in these relations is unclear because macropores and micropores, which constitute the total porosity, have different effects on mechanical properties. Therefore, the change of mechanical properties with total porosity was determined as a function of macroporosity and corresponding cell wall strength in the present study.

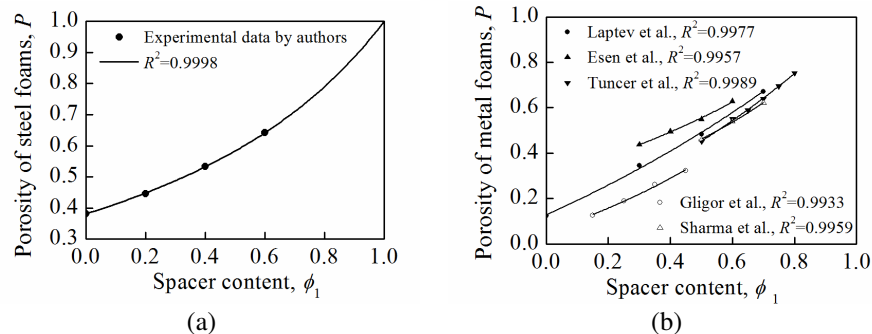


Fig. 1. The nonlinear relationship between spacer content and porosity of metal foams obtained from (a) authors' experiment and from (b) literatures.

Production of steel foams via space holder technique was employed by utilizing ammonium bicarbonate particles as space holder. Three different amounts of ammonium bicarbonate were measured as a volume fraction of mixed powders, namely, 20 vol.%, 40 vol.% and 60 vol.%. Sintering was carried out in high purity argon environment at 1200 °C, followed by furnace cooling. For steel foams with different volume ratios of steel : ammonium bicarbonate, i.e. 100:0, 80:20, 60:40 or 40:60, the measured porosities vary from 38.7% to 66.7%. The porosity is referred to the ratio between the volume of inner pores and total volume of steel foams. The inner pores were composed by macropores, obtained from the removal of space holder, and micropores in cell walls. Thus, the porosity of a practical foam can be calculated, $P = (V_1+V_2+\Delta V_1+\Delta V_2)/(V_1+V_2+V_3+\Delta V_1+\Delta V_2)$, Where, P is porosity; V_1 , V_2 and V_3 stand for the volumes of space holder, micropore in green compacts and steel powder, respectively; ΔV_1 and ΔV_2 represent the volume change of macropores and micropores during sintering, respectively. The equation can be shown as $P = (a\phi_1+b)/(c\phi_1+d)$, where $a = (1-\phi_2)R_{V1}-\phi_2R_{V2}-2\phi_2+1$, $b = \phi_2R_{V2}+\phi_2$, $c = (1-\phi_2)R_{V1}-\phi_2R_{V2}-\phi_2$, $d = \phi_2R_{V2}+1$. ϕ_1 is spacer content, $\phi_1 = V_1/(V_1+V_3)$; ϕ_2 is the micropore content in green compacts, $\phi_2 = V_2/(V_2+V_3)$; R_{V1} and R_{V2} are used to represent the volumetric change ratio of macropores and micropores, respectively, $R_{V1} = \Delta V_1/V_1$ and R_{V2}

$= \Delta V_2/V_2$. Note that the four coefficients, i.e., a, b, c, d , can be calculated based on the experimental data of ϕ_2, R_{V1} and R_{V2} . As a result, the nonlinear relationship between porosity and spacer content was obtained in theory. Then this nonlinear relationship was validated by data from authors' experiments and from literatures, as shown in Fig. 1. It can be seen that the established relationship is applicable to all ranges of porosity, irrespective of different preparing parameters.

The compressive and tensile stress-strain curves of steel foams are plotted in Fig. 2. The initial compression curves are not exactly linear. In the plastic region, curves do not show the idealized plateau stress. Because of the ambiguous transition from elastic region to plastic region, the stress at the slope intersection of these two regions is defined as the compressive yield stress (σ_{cy}). All tension curves show almost linear elastic deformation followed by plastic yielding and strain hardening up to ultimate tensile strength (σ_{ut}). After that, stress drops suddenly and the ultimate tensile strain is quite limited, especially for samples with spacer addition. It can be seen that both σ_{cy} and σ_{ut} decrease with increasing the spacer addition. A comparison of the mechanical behaviour in tension and compression indicates that the σ_{ut} are much lower than σ_{cy} . In minimum solid area models (MSA), relative properties of porous samples are equated to the fraction of solid area of the total cross section normal to the stress axis. The relation, i.e. $M^* = M_s(1-P)^n$ is utilized to account for the dependence of overall strengths of porous metals on their porosities, where P is total porosity, and n is identified as an exponent, which reflects microstructural properties the materials; M^* and M_s are defined as the mechanical properties of porous and solid material, respectively. Esen et al., using similar approach to the MSA model, modified the above equation by taking the total porosity as the macroporosity, P_{macro} , and M_s as the corresponding property of the cell wall, there is $M^* = M_{cell\ wall}(1-P_{macro})^n$. In the present study, the total porosity of steel foams without spacer addition was taken as the microporosity of cell walls of sintered samples with 20 vol.% - 60 vol.% spacer additions. Then, the macroporosity (P_{macro}) could be calculated. Fig. 3 exhibits the change of mechanical properties with $(1-P_{macro})$ term, where power law relations are obtained, i.e. $\sigma_{cy}^* = 111.7(1-P_{macro})^{2.5}$, $\sigma_{ut}^* = 58.9(1-P_{macro})^{2.7}$. It was found that the obtained proportionality constants, i.e. 111.7 MPa and 58.9 MPa, were close to the overall compressive yield stress and ultimate tensile strength of the prepared samples without spacer addition, i.e. 110.2 MPa and 57.8 MPa, which is in accordance with the modified equation based on MSA model.

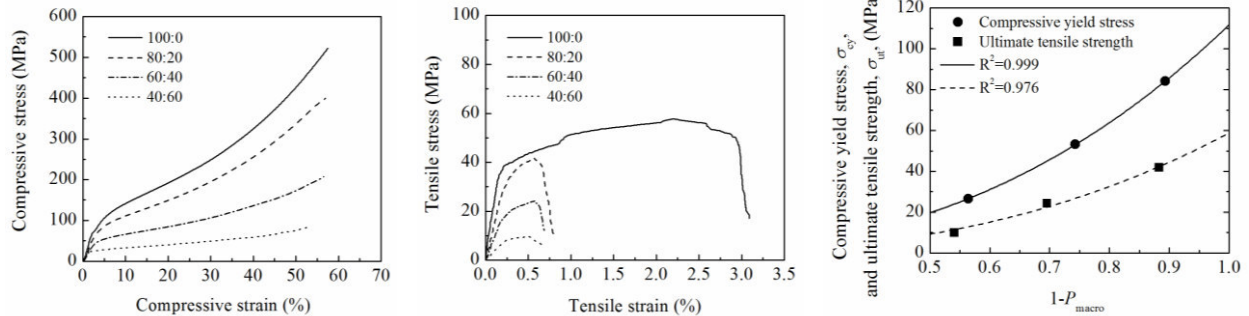


Fig. 2. Stress-strain curves of (a) compression and (b) tension. **Fig. 3.** The change of mechanical properties with macroporosity.

In conclusion, the nonlinear relationship between spacer content (ϕ_1) and porosity (P) was established based on theory when micropores in green compacts and their volumetric change during sintering were taken into account, that was $P = (a\phi_1+b)/(c\phi_1+d)$. This model equation was applicable to all range of porosity. One set of coefficients in the model equation, i.e., a, b, c, d , corresponds to a certain preparing condition, while these values changed in different preparing conditions. In addition, power law relations were obtained between mechanical properties, i.e. σ_{cy} and σ_{ut} , and macroporosity fraction, P_{macro} , in the form of $M_{cell\ wall}(1-P_{macro})^n$, similar to commonly used minimum solid area models (MSA). Moreover, it was found that mechanical properties of cell walls of porous metals produced using space holder technique can be well simulated by samples without spacer addition manufactured in the same production condition.

COMPRESSION STIFFNESS OF LEAD RUBBER BEARINGS (LRB) WITH LOW SHAPE FACTOR

Xiangxiang REN

Ph.D Candidate, Tongji University, China
tongjiren2012@163.com

Wensheng LU

Professor, Tongji University, China
wally@tongji.edu.cn

Keywords: lead rubber bearing; vertical stiffness; low shape factor

The Lead Rubber Bearings (LRB) is one type of widely used seismic isolation devices. Design formulas for vertical stiffness of LRBs already exist but do not account for the possible significant effects of central lead-plug in large elastomeric units with different shape factors. An analytical study investigating the vertical behavior of LRBs is presented and a new approximate formula for vertical stiffness is proposed. In accordance with the proposed theory, the accuracy of the formula is verified by comparison with testing results of 12 bearings with low shape factor and more than 20 bearings used in actual projects with shape factor in the range of 19.4 to 46.4. This almost covers the complete range of interest in applications of base isolation. Testing results showed good agreement with the results estimated by the proposed formula.

THE DESIGN OF AN ON-SITE EARTHQUAKE EARLY WARNING PLATFORM FOR DINSMORE BRIDGE IN BRITISH COLUMBIA

Alireza Taale

PhD Student, Civil Engineering Department, University of British Columbia, Canada
taale@ece.ubc.ca

Carlos E. Ventura

Director of Earthquake Engineering Research Facility, University of British Columbia, Canada
ventura@civil.ubc.ca

Keywords: Earthquake Early Warning Platform; Customer-oriented Deciding Concept; Writing Engineering Requirement; Sensor Network; Earthquake Detection

The study at hand outlines the definition and description of an Earthquake Early Warning Platform (EEWP) for the Dinsmore Bridge located in Richmond, British Columbia. The proposed platform is one of the deliverables defined for Dinsmore Bridge Rehabilitation Project (DBRP). The Vancouver International Airport Authority (VIAA) owns the project. The primary objective of EEWP is to ensure safe-shutdown-safe-operation of the bridge during an earthquake. The client, VIAA, requires at least 20s of warning time in order to secure the bridge and stop the inbound traffic. The study at hand demonstrates how the client's requirements translate into system engineering requirements and technical specifications.

Most contractual problems relating to performance may occur because of inappropriate drafting of the technical specifications. The problems commonly relate to: inclusion of irrelevant or contradictory information, use of ambiguous or undefined terms, or concentrating on the means by which a result is to be achieved rather than on the performance required. The designers often provide too much information for the suppliers about the conditions under which the equipment must operate. They indeed overlook the fact that this usually leads to poor flexibility of equipment or cost overrun. On the other hand, too general scope of work would likely lead to scope creep and conflict between the client and the vendor. In this study, treating this challenge is of central importance.

To effectively meet the challenge, we introduce a unique framework based on the global anatomy of the EEWPs that is consisting of: event characterization, systematic application, and data communication. The first block intends to separate the seismic event from anthropogenic vibrations and it then characterizes the dangerousness of the event. The systematic application contains the desired decision rule whether the platform should issue an alarm and perform the preventative actions. Lastly, the data communication block describes the procedure of packaging and dispatching the information to the client(s). The proposed framework facilitates the decomposition of each block into a set of prime modules. It then ensures each module delivers to the client's requirements in an effective and efficient manner. We name the proposed framework as the Client-oriented Automatic Deciding Concept or *Cadence* in short. The following diagram displays the flow of information within the *Cadence* framework:

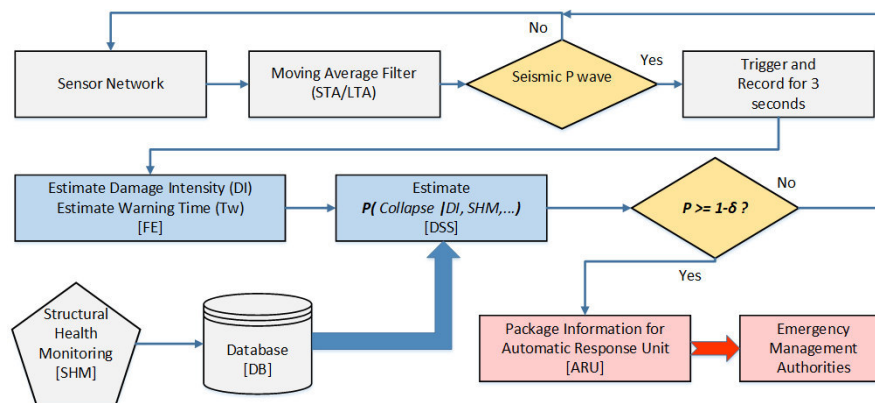


Figure 1. The graphic representation of the information flow within the *Cadence* framework. The grey, blue, and pink modules respectively represent the three global building blocks of the EEWP. The parameter δ represents an arbitrary confidence level and it is at client's discretion. It takes on values such as 0.1, 0.01

We design each module in Figure 1 in order to: carry out the assigned task in an autonomous manner, be fast and reliable, have minimum cost, and upgrade without compromising the performance of the adjacent modules.

Once the platform detects the presence of seismic P wave, feature extractor module (FE) extracts the features of interest to characterize the event. These features include but not limited to damage intensity (DI) and epi-central location (R) of the unfolding earthquake. The DI is the absolute value of the inner product of acceleration (\mathbf{a}) and velocity (\mathbf{v}) with *cgs* unit in *log10* scale. The inner product is indeed a physical variable that represents the delivered power per unit of mass ($\frac{Watt}{Kg}$). According to previous studies, this quantity can be estimated in real time and its value increases immediately after P wave arrival. More importantly, the DI can correspond to Modified Mercalli Intensity (MMI) scale with no need to estimate the magnitude and location of the earthquake.

The available early warning time merely depends on the earthquake location, assuming a uniform P wave velocity model from the source to the site. We may consider the alarm generated by EEWS effective or useful if and only if two conditions hold. First, the warning time T_w at a site is long enough for useful mitigation actions to be undertaken, i.e., larger than some critical value T_c . Secondly, the observed shaking intensities are recognized to be strong enough for probable serious damage, i.e., they exceed a critical value I_c . The critical value for time depends on the extensiveness of mitigation measures. On the other hand, the value of I_c depends on the dynamic properties of the structure, site class, regional seismicity, and state of health of the structure when event occurs. These pieces of information reside in the database module (DB) and update periodically. Subsequently, the decision support system module, i.e. DSS, estimates the conditional probability of collapse. Therefore, the proposed system is able to classify the seismic event prior to the arrival of damaging waves. The final decision is whether the bridge may safely remain in operation or deny the inbound traffic.

In Figure 2, we described the overall configuration of the EEWP for DBRP. We recommended two sets of downhole arrays, each consisting of at least one Power over Ethernet (PoE) accelerometer. The detailed description of the configuration is outside the scope of this extended abstract but some unique features of the design are worth mentioning.

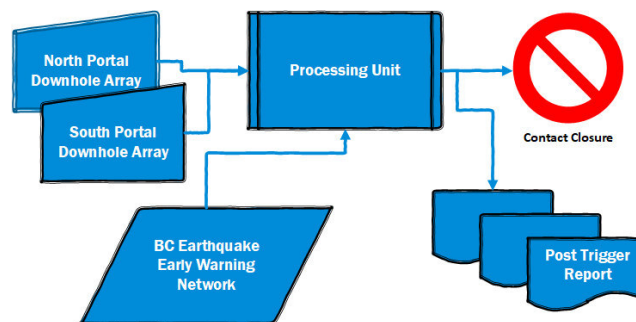


Figure 2. Dinsmore Bridge Earthquake Early Warning System Overall Configuration

The proposed system for DBRP is classified under the on-site earthquake early warning platforms. The system independently performs; however, it is capable of negotiating the final decision with the outside world. We choose to employ very basic detection and event characterization algorithms, i.e. STA/LTA and Damage Intensity. This selection facilitates the implementation and the troubleshooting of the system; nonetheless, future enhancement is also quite doable because of the modular design of the Cadence platform.

In order to manage client’s expectation, we associate a likelihood to the requirement of generating 20s warning. Based on the seismicity of the region and the site-structure properties, the disaggregated distance for the hazard level of 2% in 50 years results in 4% probability of exceeding the 20s requirement. In other words, it is highly likely that the damaging event occurs at a location within 100km of the site, assuming $5 \frac{km}{s}$ for the P wave velocity.

Our future work will include the implementation of the selected algorithms as well as the underlying hardware. We also aim to test multitudes of algorithms and configurations in order to identify an optimal solution for an on-site earthquake early warning platform.

SEISMIC RELIABILITY OF STRUCTURES CONSIDERING SPATIAL VARIABILITY

Jingran He

School of Civil Engineering, Tongji University, Shanghai, China
hjrymy@gmail.com

Jianbing Chen and Jie Li

School of Civil Engineering & State Key Laboratory of Disaster Reduction in Civil Engineering, Tongji University, Shanghai, China
chenjb@tongji.edu.cn

Keywords: Seismic reliability; Spatial variability; Random field; Probability density evolution method.

The seismic performance of a structure could be quantified by the seismic reliability of the structure. In most of the existing investigations, the seismic action was regarded as a random excitation but the randomness of structure itself was neglected. However, in reality the structures are random-parameter systems rather than deterministic system. Some researches have been done to reveal that the coupling effect of the randomness of structural properties and excitation will greatly affect the performance of structures. In these studies, the randomness of structural material parameters are usually modelled by random variables with-out spatial correlation. However, the construction process of structures implies that proximity of materials exists, and thus the spatial correlation exists in the structures. In this paper, the material parameters of a 7-story concrete structure are considered as random fields using the Stochastic Harmonic Function. An elastoplastic damage constitutive law of concrete is applied, and the seismic reliability is assessed by using the Probability Density Evolution Method.

The Stochastic Harmonic Function (SHF) is firstly proposed to represent the random field, the accuracy of this method is proved to be higher than the spectral representation (SR). For example, the one-dimensional PDF of the SHF field is much closer to the target standard Gaussian distribution than the SR field. The result is shown in Fig. 1.

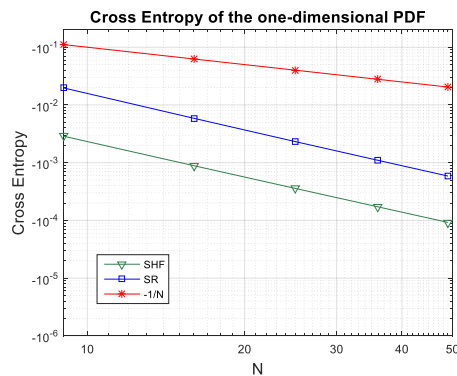


Fig. 1 The cross entropy of SHF and SR

Then the SHF field is applied to represent the concrete properties in the shear wall of a 7 story model. The model is a test model in a shake table test performed in UCSD. The seismic reliability of the model is analysed by the Probability Density Evolution Method (PDEM). For different correlation length, the reliability and the failure mode of the model are different as shown in Fig. 2 and Table 1.

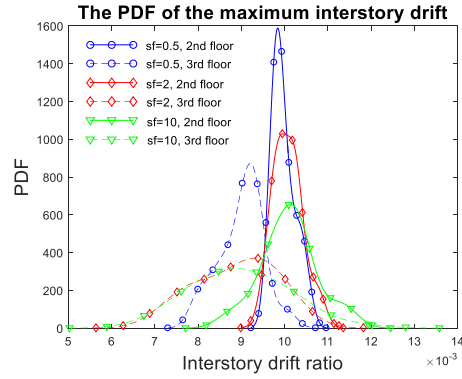


Fig. 2 The PDF of the maximum inter story drift

Table 1 The failure probability of the 2nd and the 3rd floor

| Scale of fluctuation | Probability of failure – 2nd floor (Pf-2) | Probability of failure – 3rd floor (Pf-3) |
|----------------------|---|---|
| sf=0.5m | 0.39536 | 0.03019 |
| sf=2m | 0.55300 | 0.14451 |
| sf=10m | 0.57194 | 0.20373 |

The seismic reliability of the structures with spatial variation differs from each scales of fluctuation. The reliability drops as the scale of fluctuation growing. The increase of the scale of fluctuation results in the increase of the coefficient of variation of the structures' response. The combination of these two effects finally cause the variation in the failure mode. From this point of view, the seismic performance of a structure should be evaluated by a model with spatial variation, and the correlation relationship along the space should be further investigated.

REALIZATION OF FABRICATED CLT PANEL STRUCTURE

Yijie SONG

Graduate student, Tongji University, China
songyijie123@tongji.edu.cn

Haibei Xiong

Professor, Tongji University, China
xionghaibei@tongji.edu.cn

Keywords: CLT, timber structure, prefabricated; modularization, plates structure, sustainable requirement

Cross-laminated timber (CLT) is widely used in European and North American as a new kind of wood material. CLT plate is suitable for the production of prefabricated components in modularization architecture. The Otto Cafe is the realization of the concept of prefabricated modular timber structure that is the first prize work of Timber Structure Design Competition. CLT plates of 3.6m×3.6m basic size can be bearing structure material. Six reasonable structure models were select in view of the requirements of architecture, reciprocal structure concept and finite element analysis. Structural response calculations and checking computations was competed until meeting the code requirements. The displacement of structure is main controlling factor. The manufacture of joints is a crucial part of the construction. Otto cafe can realize space variation and industrialized production by means of prefabricated construction to meet various demands and realize the sustainable requirements of energy conservation and environmental protection.

CYCLIC PERFORMANCE OF NON-SEISMICALLY DESIGNED RC BRIDGE PIERS REPAIRED AND RETROFITTED WITH GFRP

Mosharef HOSSAIN

MASc Student, University of British Columbia, Canada
mosharef.hossain@alumni.ubc.ca

Shahria ALAM

Associate Professor, University of British Columbia, Canada
shahria.alam@ubc.ca

Keywords: Deficient Bridge Pier, Cyclic Loading, GFRP Confinement, Repairing, Retrofitting.

An experimental investigation is presented in this study on seismic performance evaluation of circular RC bridge pier repaired and retrofitted with GFRP confinement. Before the implication of seismic design code, most of the bridge piers were not designed with sufficient lateral confinement. To simulate that kind of situation, two bridge piers were initially designed without following the seismic and bridge design codes that literally had no confinement from transverse reinforcement. These piers after testing in as-built condition, were repaired and retrofitted at two different loading stages- one before and the other one after earthquake has hit and caused damages to the pier. The piers were tested under quasi-static reverse cyclic loading following a standard loading protocol with post-tensioning on top to mimic the effect of axial load. Dynamic behavior of the column was ignored in this study. Before applying confinement to the piers, cylinders confined with different thickness of GFRP were tested to find out the effect of GFRP confinement on the compressive strength of concrete. This study presented here also makes use of recent advances in real-time testing hardware to investigate the effects of lateral cyclic load on the structural response of non-seismically designed, GFRP repaired, and retrofitted RC bridge piers. A pioneering test setup in which hydraulic actuator is controlled at precise loading rate was used to test the piers until failure. The experimental challenges and piers behavior are discussed. Both the repaired and GFRP retrofitted piers showed improvement in lateral load carrying capacity by 24% and drift capacity increased to 6.9%.

A NEW ENERGY DISSIPATION BAR AND ITS APPLICATION

Ye Liu

Ph.D candidate, Southeast University, China
dnluiye@126.com

Chun-Lin Wang

Associate Professor, Southeast University, China
email. chunlin@seu.edu.cn

Keywords: low-cycle fatigue; aluminum alloy; bamboo-shaped; buckling-restrained braces

1. INTRODUCTION

Problems of the existing energy dissipaters studied above cannot be neglected, which can be addressed as follows:

(1) Premature buckling. The fuse-type mild steel replaceable dissipater discussed by Sarti et al. showed stable hysteresis in tension, but buckled in compression at relatively low displacements even if epoxy or grout was filled into the confining tube.

(2) Limited configurations in structures. The fuse-type dissipater can only effectively work in tension based on the experimental results, which largely limits the practical configurations of the fuse-type dissipater constructed in structures to horizontal or vertical directions.

(3) Difficult grouting. The dimensions of energy dissipaters are relatively small, which requires high precision of mechanical working. Besides, the relatively small clearance between the fused bar and the confining tube directly affects the compaction degree of filled materials, which is a major concern to guarantee the high performance of the energy dissipater. In that way, the quality of the grouting can be difficult to be controlled.

Problems addressed above are urged to be solved to enrich the application of energy dissipaters in precast structures. A more comprehensive study on the style and adopted material of energy dissipaters has not formed until now, and a wider range of geometric and mechanical parameters of energy dissipater should be covered. The more testing data related to energy dissipaters are necessary to create a parametric analysis and provide preliminary guidelines for the design of the dissipaters.

2. SPECIMEN SELECTION AND CLASSIFICATION

2.1 Configuration of aluminum alloy bamboo-shaped fuse-type energy dissipater

Referring to Figure 1, the new aluminum alloy bamboo-shaped fuse-type energy dissipater (BFED) consists of an inner bamboo-shaped core and an outer circular tube. Typically, the core is composed of a succession of slubs, segments and transition zones depicted in Figure 1(a), where slubs are designed to control the deformation pattern of the core. The transition zone is set between the segment and the fixed end to spare enough space for the actuator moving back and forth. In the middle slub, an opening with a radius of 1.5mm is prepared for the stopper pin which is made of a nail with a radius of 1.4mm and length of 40mm, preventing the relative movement between the core and the tube in the longitudinal direction during tests. The red paint is employed on the surface of segments to apparently show any possible contact between segments and the tube. From the cross-section details of the BFED shown in Figure 1(b), it is found that the core is surrounded by the tube, and small gaps, d_1 and d_2 , are respectively provided between the slub and the tube and between the segment and the tube.

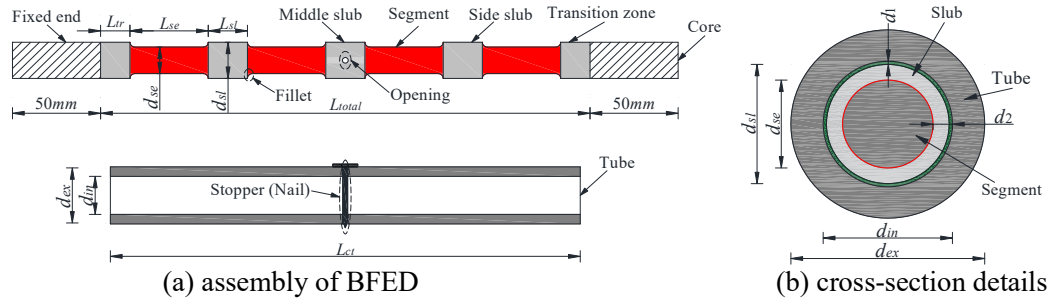


Figure 1. Details of BFED: (a) assembly of BFED and (b) cross-section details.

2.2 Test results

All testing specimens demonstrate stable and repeated hysteretic capacity, without any local and overall buckling during loading histories even at the maximum strain amplitude. Test results of all specimens are summarized in Table 1.

Table 1. Test results of BFED specimens

| Series | Specimen | $\Delta\varepsilon$ (%) | N_f | n_i | CID (%) | CED (N·m) | Contact conditions | Loading patterns |
|--------|------------------|-------------------------|-------|-------|---------|-----------|--------------------|------------------|
| S1 | S1-L40S20G1-C1 | 0.57 | 53 | - | 69.1 | 2657.5 | No | CSA |
| | S1-L40S20G1-C2 | 0.86 | 23 | - | 76.0 | 4404.9 | No | CSA |
| | S1-L40S20G1-C3 | 1.14 | 7 | - | 37.1 | 2539.4 | No | CSA |
| | S1-L40S20G2-C1 | 0.57 | 79 | - | 103.0 | 4181.4 | No | CSA |
| | S1-L40S20G2-C2 | 0.86 | 24 | - | 79.3 | 4713.0 | No | CSA |
| | S1-L40S20G2-C3 | 1.14 | 6 | - | 31.8 | 2219.8 | No | CSA |
| S2 | S2-L40S5G1-V | - | - | 14 | 39.8 | 3385.4 | No | VSA |
| | S2-L40S5G1-V(6) | - | - | 12 | 35.8 | 4966.6 | No | VSA |
| | S2-L60S5G1-V | - | - | 20 | 51.7 | 6615.6 | Yes | VSA |
| | S2-L80S20G1-V(2) | - | - | 12 | 35.8 | 2951.5 | No | VSA |
| | S2-L40S20G1-V | - | - | 20 | 51.7 | 4671.3 | No | VSA |
| | S2-L60S20G1-V | - | - | 14 | 39.8 | 5391.1 | No | VSA |

Note: N_f is number of failure cycles; n_i is number of cycles at additional constant strain amplitude; CID is cumulative inelastic deformation; CED is cumulative energy dissipation.

3. Conclusion:

In the present study, 12 specimens in all were tested to investigate hysteretic behaviors of BFED and develop high performance energy dissipaters, while design parameters of these specimens were compared to provide an effective way to fabricate new BFED specimens. The main results are summarized as follows:

1. On the basis of the test results, all BFED specimens show stable and repeated hysteresis loops without any local and overall buckling even at the maximum strain amplitude. The failure of BFED is resulted from the fatigue of material.

DISPLACEMENT BASED-DESIGN OF CONCRETE-CLT HYBRID BUILDING

Jayanthan MADHESWARAN

MASc Student, The University of British Columbia, Canada.

jayanthan.madheswaran@alumni.ubc.ca

Solomon TEFAMARIAM

Professor, The University of British Columbia, Canada.

solomon.tesfamariam@ubc.ca

Keywords: RC-CLT hybrid building; Passive energy dissipation device; Displacement based-design.

Introduction

Cross Laminated Timber (CLT) is found to be an effective material for resisting the lateral forces because of its high strength and stiffness. Considering the advantages of CLT, the researchers at UBC have developed an innovative steel-timber hybrid system by using CLT as an infill wall with bracket connections to enhance the performance of steel moment frames. In this paper, a concrete-CLT hybrid system is developed. This system consists of reinforced concrete frame with CLT panel and steel slit damper. The steel slit damper is used as a connecting element between the CLT panel and RC beam. Initial study has been conducted to find the appropriate geometry combination of the damper which can provide low stiffness and high energy dissipation. Then, to assess the performance of this proposed hybrid concept, a single storey single-bay RC frame with the hybrid concept were modeled using OpenSees program. The model was subjected to monotonic pushover analysis and the result clearly indicates that the use of damper to connect the wall enhances the load carrying capacity of frame by maintaining global ductility. Further, the use of force based design guidelines for finding the inelastic design force is not possible because over strength and ductility factors are not established for this system. Therefore, this study developed a direct displacement based-design procedure for this hybrid system to calculate the lateral forces. The validation of this design framework is still under research.

Modeling of Concrete-CLT

In this work, to understand about the overall performance of the proposed hybrid system shown in Figure 1a. Initially, a bare RC frame dimensions and cross section of the elements were obtained from the previous research and it is validated with their experimental work using OpenSees model. Then, the frame dimension was scaled three times the original size to accommodate the CLT panel. In this system, the CLT panel width is reduced to 50% of the frame width to avoid the pre-mature shear failure of the columns. The panel is connected to the RC beam using the three steel slit dampers at the top, and bottom is connected to three rigid hold-downs to avoid the out-of-plane failure. Further, the steel slit damper is selected with the yield force of 40 kN and stiffness 16 kN/mm by considering the damper behaviour with the RC frame. The optimal geometry and their corresponding performance of the damper selection was studied in the authors previous work using ABAQUS program.

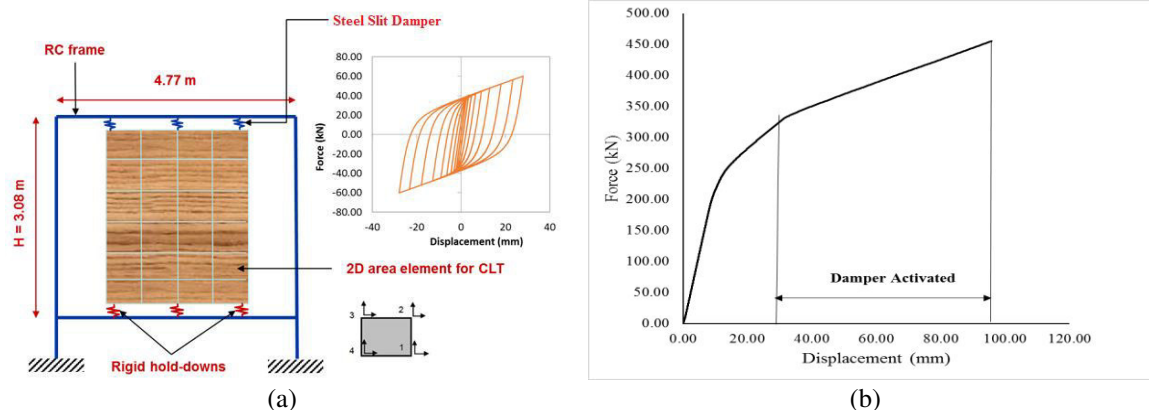


Figure 1 CLT-RC hybrid system: (a) Test model and (b) Monotonic pushover result

The numerical modeling is carried out using OpenSees program. The beam and columns were modeled as force-beam column element using distributed plasticity approach. Steel and concrete were assigned with Uniaxial material properties in OpenSees. CLT panel was modeled as a quad element with linear elastic-isotropic wood material property. The damper and rigid hold-downs are modeled as two node link elements with Uniaxial Steel02 and rigid material respectively. The developed model was subjected to monotonic pushover analysis to monitor the performance. The preliminary result indicates that the damper connection activated in the proposed model and enhances the load carrying capacity by maintaining the ductility of the system (Figure 1b).

Direct Displacement Based-Design Framework for Concrete-CLT hybrid building

Direct displacement based-design was first introduced by Priestley in 2003 for reinforced concrete building. This design methodology is developed based on the fixed target displacement as the response parameter. Considering the advantages of this method than the force based design procedure, researchers have proposed the displacement based design framework for different structural systems. The displacement based-design framework developed for the concrete-CLT with damper connections is shown in Figure 2.

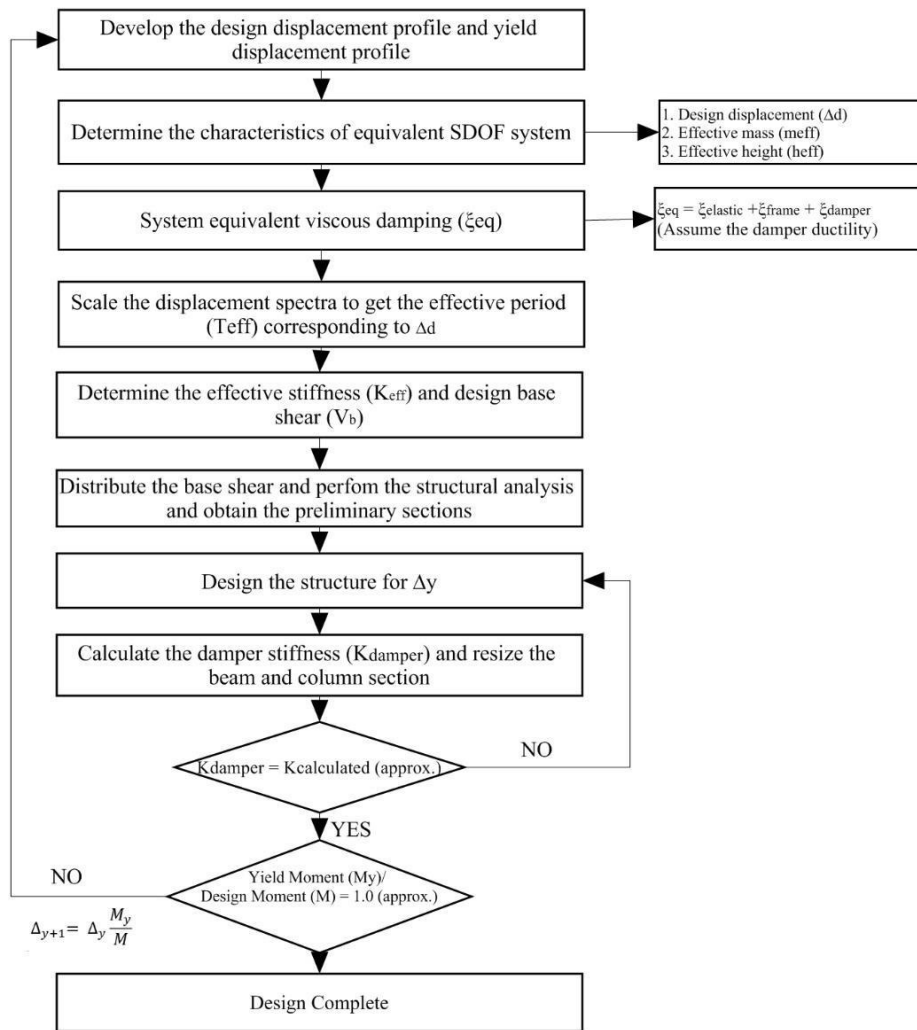


Figure 2: Direct displacement based-design framework for Concrete-CLT hybrid building

Conclusions

Based on the pushover results, the system equipped with damper exhibited a good performance in terms of strength. This paper also presented a displacement based design framework for this hybrid system. Further, the future research aims to validate the proposed design framework by performing a nonlinear time history analysis.

EXPERIMENTAL RESEARCH ON THE SLIDING ANTI-TENSION STEEL DAMPING DEVICE

Hao Gao

Doctoral candidate, Tongji University, China
001gaohao@tongji.edu.cn

Junjie Wang

Professor, Tongji University, China
jjwang@tongji.edu.cn

Keywords: sliding; anti-tension; shear failure; hysteretic energy consuming performance; low-cycle fatigue life;

Bridge structure places the special demands on steel damping devices: (i)The damper have the ability to slip in a certain amount without force generated under temperature load; (ii)In some cases, for example, when bridge structure is subjected to vertical ground motion, the damper is required to have tensile resistance. In order to adapt to the special requirements for bridge structure, a sliding anti-tension steel damping device is designed. Its hysteretic energy consuming performance, low-cycle fatigue life and tensile strength are proved by the full-scale experiment. And the constitutive model of steel damping device can be obtained based on the experiment results. By the numerical simulation of earthquake response for a 3-span continuous bridge taking account of bearing shear failure, the influence of steel damping device on the displacement of girder and the endurance of pier are analyzed, and the effectiveness of the proposed steel damping device is verified.

The design procedure of self-centering precast walls based on DDBD

Liumeng QUAN

PHD candidate, Tongji University, China
cherry_ari@163.com

Xilin LU

Professor, Tongji University, China

Keywords: self-centering; post-yield stiffness; mild steel moment ratio; equivalent viscous damping; design example; static analysis; dynamic analysis

Damage investigations after the strong earthquakes show that the existing seismic design method is capable to prevent the structures from collapse. However, the economic lost is still huge due to the downtime and reconstruction cost. Self-centering wall structure is a kind of resilient structures, which draws extensive attention recently. The self-centering wall with only one rocking joint at the base panel experiences decompression, yielding, prestressing tendons(PT) tendons yielding and the toe concrete crushing subject to push loading. The directly displacement-based design (DDBD) is a reliable design method, which converts a multi-degree of freedom system to a single-degree of freedom system. The equivalent viscous damping ratio, the post-yield stiffness ratio and the scant stiffness are main factors in the joint design process. The equivalent viscous damping ratio is important in the procedure of achieving the suitable elastic displacement spectrum. The Ring-Spring hysteretic rule is appropriate for self-centering structures and the corresponding equivalent viscous damping ratio is related with ductility factor, post-elastic stiffness ratio and energy dissipation coefficient. The equivalent hysteretic viscous damping ratio formula is acceptable without considering the energy dissipated by toe crushing when compared with experiment data. The area of PT tendon and the debonded length are the main factors for post-yield stiffness. The former formula generally overestimates the post-yield stiffness of the precast walls with relative high axial load ratio and mild steel because $P-\Delta$ effect and increasing contact length not in consideration. The experiments, including with or without additional axial force and mild steels, conducted by Rahamn and relevant experiment data verify the conclusion. The case study building is an eight -story PSFW structure, designed according to the DDBD approach mentioned before. The seismic fortification intensity of the building site is assumed to be 8. The seismic site design is Group 2 and Site Class II and the characteristic period is 0.40s. In this article, 3 cases are used to illustrate and validate the joint design procedure after DDBD. The design background including loads and materials are identical. The only difference between the 3 cases is the performance level requirements. The serial number 1/2/3 is the corresponding number represented the performance level: CP, LS and OC. The equivalent viscous damping ratio is assigned to the case 1/2/3 respectively. The first phrase is preliminary for section geometry design. The second phrase is making sure the moment capacity of the joint, including the moment contributed by PT tendons, axial load and mild steel. The last phrase is making sure no toe crushing before the ultimate drift and the elongation of PT tendons, mild steel in a certain range. The post-yield stiffness and the contact length are also considered for design verification. Both the static and dynamic analyses are conducted in OpenSEES software. The ultimate moment capacity and energy dissipation capacity is verified under cyclic loading. In addition, 6 earthquake waves are selected and the peak acceleration is uniformed to 400cm/s^2 . The result is a little conservative and acceptable.

PERFORMANCE EVALUATION AND STRUCTURAL DESIGN OF RACK CLAD BUILDINGS

Peng Zhang

PhD Candidate, University of British Columbia, Okanagan, Canada
p.zhang@alumni.ubc.ca

M. Shahria Alam

Associate Professor, University of British Columbia, Okanagan, Canada
shahria.alam@ubc.ca

Keywords: Rack clad building; Perforated columns; Buckling failure; Seismic Design

Pallet Rack Structure (PRS) features high capacity to weight ratios, short construction periods, and good salvage values. Figure 1 shows a unit of PRS. It has been widely used for storage in a commercial or industrial building (e.g., shop Costco). In the cross-aisle direction, PRS forms braced frames to resist lateral loads while in the down aisle direction semi-rigid frames are used. When a PRS is built independently (without an exterior structure) and clad in walls and a roof, it becomes a Rack Clad Building (RCB) or rack supported building. An RCB is presented in Figure 2. RCB is more economical compared with PRS, and consequently, it is gaining more attraction to the customers. The columns, beams, base plates, and connectors are thin-walled cold-formed elements. They can be prefabricated at a factory and delivered to a construction site for a quick assembly. Hook-in end connectors are welded to the beam ends so that the beams can be easily mounted on the columns. Under this circumstance, welding and bolting are not necessary, and the floor levels can be easily adjusted, which greatly facilitate the assembly. The drawbacks of RCB are a low lateral stiffness in the down aisle direction, and the columns are slender and prone to a buckling failure. To date, there are no proper design guidelines for RCB, and the research is in an infant stage. These make the threats to RCB from earthquakes prominent; therefore, the development of seismic design guidelines for RCB is crucial.

The presentation consists of the following two topics:

(1) The development of an analytical design methodology for predicting the buckling capacity of perforated rack columns under an uniaxial compression load.

Rack columns with perforations are prone to buckling failures, e.g., local buckling, distortional buckling, and global (flexural or torsional-flexural) buckling. The buckling modes are dependent on the columns' slenderness, and for the lengths where buckling modes transition happens, two or three modes interaction may occur. In this research, three types of perforated rack columns were experimentally tested, see Figure 3 for example. The specimens consisted of seven different lengths that were ranging from 250mm to 2100mm, which capable of exploring all the buckling modes. Direct Strength Method (DSM), proposed by Moen and Schafer (2011), has been incorporated in the North American design standard AISI S100 (2006) for predicting the compression capacity of perforated lipped channels. The DSM has been evaluated and proved to be not accurate for the rack columns; therefore, a modified DSM has been developed in this research. Moreover, numerical simulations were conducted by using a finite element software, ANSYS, to predict the columns' buckling response, and the results were consistent with the experimental data.

(2) Evaluation of the seismic behaviour of rack clad buildings and the development of seismic design guidelines.

Under earthquakes, RCB may suffer larger lateral deformations (drifts). The deformation can impose significant $P-\Delta$ effects to the columns, which may induce columns buckling and further trigger a structure collapse. Literature shows under earthquakes, the plastic deformations of RCB were concentrated at the base plates and the beam-column connections while the beams and columns were maintaining elastic. The beam-column connections play a major role in providing the lateral stiffness for the frame and dissipating seismic energy. Nowadays, most researches conducted for designing structures against earthquakes are based on numerical simulations where earthquake records are input as an exterior load. For the numerical models representing a full-scale structure, spring elements are employed to model the beam-column connections for convenience. Consequently, a reliable constitutive model of the connections is indispensable for the numerical simulations. In this research, three different types of beam-column connections will be experimentally tested under quasi-static cyclic loads. The testing prototype is shown in Figure 4. The moment-

rotation hysteretic loops will be captured and used to generate the constitutive models. These models will be incorporated in the full-scale RCB models to run an enormous amount of seismic simulations. Based on the simulation results, the seismic performance of RCB can be evaluated, and the seismic design guidelines can be developed.

Developing seismic design guidelines for rack clad buildings is a long-term goal of the research group. The work carried out by the authors will provide an effective and efficient tool (analytical design methodology) for structural designers to predict the rack column capacity and optimize their designs afterward. This tool has a great potential to make the experimental test of rack columns unnecessary. A preliminary seismic design guideline will be developed, which will greatly reduce the seismic threats and improve the safety for rack clad buildings.

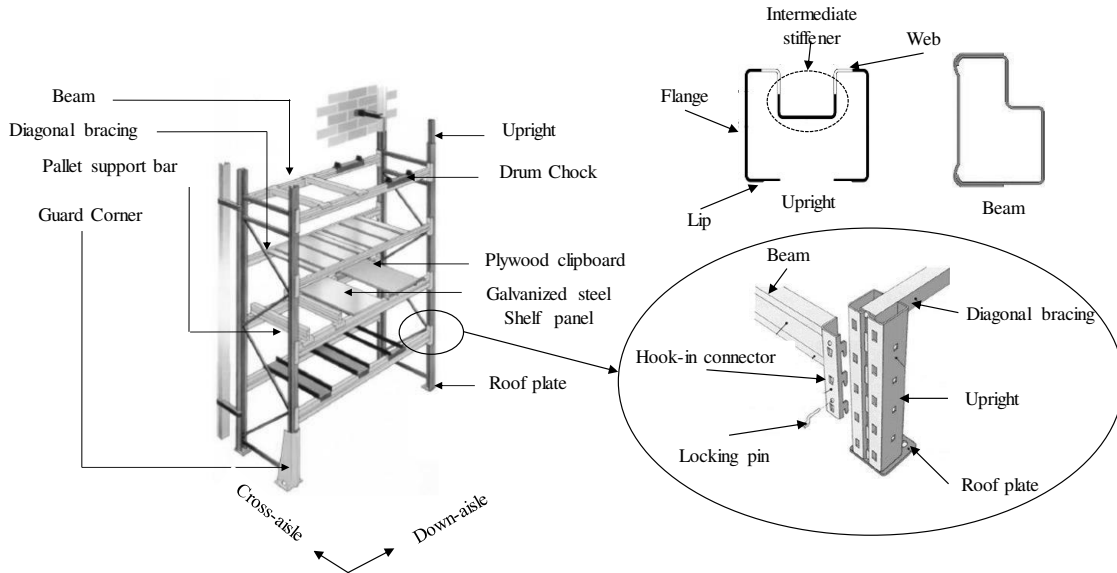


Fig.1. A unit of PRS/RCB



Fig.2. An RCB under construction

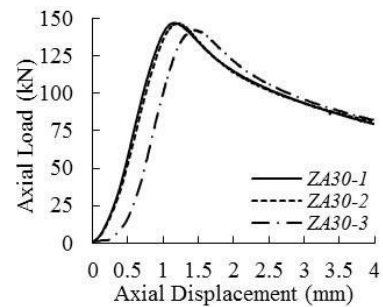


Fig.3. Rack column testing setup and load-displacement curve

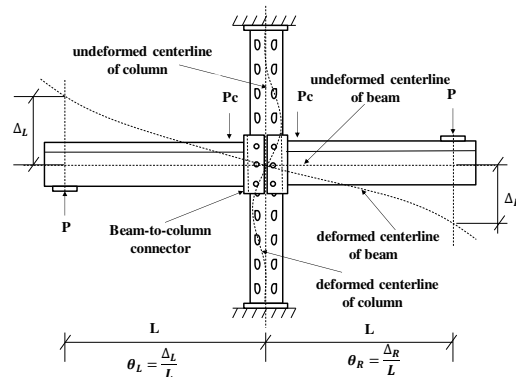


Fig.4. Column-beam connection testing setup

PERFORMANCE BASED DESIGN OF ROCKING WALL WITH BRBS IN BASE

XIAOYAN YANG

PhD Candidate, Southeast University, China
yangxiaoyan@cau.edu.cn

JING WU

Professor, Southeast University, China
seuwj@seu.edu.cn

Keywords: Rocking wall; Buckling-Restrained Brace; Performance-Based design; Strand with gap

Rocking Wall with BRBs in Base (HWBB) can rock around the pin at the middle bottom of the wall and BRBs are installed at the two-side bottom of the wall. Strands with gaps are placed symmetrically at the two-sides of rocking wall and can prevent the collapse of HWBB under quite rare earthquake due to P- Δ effect, providing tension force to form the resistant moment with the compressed BRB. This kind of structure conforms to the resilient concept, which can restore the function after earthquake. The rocking wall can remain elastic during the earthquake, while seismic energies are all dissipated by BRBs and only BRBs need to be replaced after earthquake.

Performance Based Design will be used to design HWBB, in which the stiffness of wall, the area of BRB and the length of BRB are parameters used for design. Direct Displacement-Based Design method will be used. Different performance objectives will be set according to different seismic levels. For minor earthquake level, the BRBs should remain elastic; for moderate earthquake level and rare earthquake level, BRBs will yield and dissipate seismic energy; for very rare earthquake level, the strand with gaps will begin to work and the area of strand and the length of gap in the strand need to be designed.

The seismic performance of HWBB can be evaluated by indexes such as interstory displacement, top displacement, interstory drift, DCF and so on.

A SYSTEMATIC EXPERIMENTAL STUDY ON THE OPTIMIZATION OF STEEL-MICROFIBER REINFORCED CONCRETE

Yi Xiao

Doctoral student, State Key Laboratory of Disaster Reduction in Civil Engineering, Tongji University, China
yixiao@tongji.edu.cn

Ying Zhou

Professor, State Key Laboratory of Disaster Reduction in Civil Engineering, Tongji University, China
yingzhou@tongji.edu.cn

Keywords: steel-microfiber reinforced concrete; optimal type; dispersion; workability; mechanical property

To maximize the potential of steel fiber (S) and microfiber blends in a concrete matrix, the optimal type of the fibers was first investigated in this paper through a systematic experimental study comparing four types of steel-microfiber reinforced concrete. The microfibers considered include microfilament steel fiber (MS), polypropylene (PP), polyvinyl alcohol (PVA) and polyacrylonitrile fiber (PAN). The dispersion of the fiber, workability and mechanical property of the concrete matrix were evaluated. The experimental results of dispersion and workability indicate the following similar priority sequence: MS>PVA \approx PP>PAN. For the mechanical property, S-MS and S-PVA reinforced concrete generate an overall higher enhancing effect than S-PP and S-PAN with a positive hybrid effect in most properties. S-MS is superior in strength, and S-PVA is effective in improving the toughness. Because PVA has relatively good dispersion and workability, and toughness is the most important and effective mechanical property in fiber-reinforced concrete, this study recommends that S-PVA is the best type of steel-microfiber reinforced concrete.

EXPERIMENTAL STUDY OF A NEW BEAM-TO-COLUMN CONNECTIONS FOR PRECAST CONCRETE FRAMES USING HIGH- STRENGTH BARS IN THE BOTTOM

Hui Yang

Doctor, Southeast University, China
93897202@qq.com

Zhengxing Guo

Professor, Southeast University, China
Guozx1956@126.com

Keywords: beam-to-column connection; precast concrete frame; high-strength bars; cyclic loading

A new beam-to-column connection developed for precast concrete-resisting frames was proposed in this article. This connection could be constructed easily and rapidly, and it also avoided reinforcement congestion or obstruction in connection regions by using minor diameter high-strength bars which could be bent by hand.

Four full-scale beam-to-column connections, including a monolithic specimen, were tested to evaluate the earthquake resistance under reversal cyclic loading. One precast specimen was manufactured following all the proposed details. For comparison purpose, the other precast specimens were made without one or two structural details like additional small size stirrups in the bottom of the U-shaped hollow and using high-strength longitudinal bars at the top of beams.

After analysis on the hysteretic behaviour, strength, deformability, stiffness, and energy dissipation, it was showed that the proposed connection exhibited good seismic resistance, thus could be used in seismic regions. Furthermore, the existence of additional stirrups enhanced energy dissipation and ductility, while the use of high-strength longitudinal bars decreased the energy dissipation capacity and improved the ductility.

EXPERIMENTAL AND NUMERICAL INVESTIGATION ON EXISTING BUILDINGS' DIAPHRAGMS PERFORMANCE

Niels Juhl Savnik

Master student, University of British Columbia, Canada and Technical University of Denmark, Denmark
S123685@student.dtu.dk

Carlos E. Ventura

Professor, University of British Columbia, Canada
ventura@civil.ubc.ca

Evangelos Katsanos

Asst. Professor, Technical University of Denmark, Denmark
vakat@byg.dtu.dk

Rune Brincker

Professor, Technical University of Denmark, Denmark
runeb@byg.dtu.dk

Sandro D. R. Amador

Postdoc, Technical University of Denmark, Denmark
sdio@byg.dtu.dk

Freddy Pina

Dr, PBRV Consulting Ltd., Canada
fpina@pbrvconsulting.com

Keywords: Ambient Vibration; Operational Modal Analysis; Diaphragm performance; FEM updating;

Objectives

A large number of existing structures as buildings, bridges and other infrastructures, have decreasing performance, and it is very uncertain to predict the capacity with confidence for the rest of the service life. Based on this, it is a high priority for the engineering society to identify the real performance of structures, when they are exposed to different types of effects. This is the only way to precisely predict the current capacity of the structure, and evaluate the opportunity for retrofitting, if necessary. Within this framework, the aim of this master project is to identify the horizontal movements of existing reinforced concrete structures exposed to wind loads, earthquake loads and ambient vibrations. Primary there is a gap in the literature related to studies concentrate on horizontal movements of diaphragms, and this incomplete knowledge have already lead to simplified models, which cannot predict the precise horizontal movements. Thereby is it anticipated, this integrated research project, which includes both an experimental and numerical part, will contribute with the necessary knowledge to predict the horizontal movements of a building. More specific the aim of the research project is to understand the horizontal behavior of high-rise buildings, by investigating the movement of the

horizontal diaphragms, and performing a nonlinear dynamic analysis of the storey diaphragms. The emphasis of the project is to clarify the diaphragm effect in relation to horizontal behaviour in high-rise buildings. The investigation of the diaphragm effect embrace acquiring ambient vibration accelerations from the horizontal movement of a high-rise building, placed in Vancouver Canada, and comparison with a comprehensive highly nonlinear 3D Finite Element Model of the high-rise building. A part of the preliminary work contains a careful study of the modelling process and the Rayleigh-Ritz method. The diaphragms are modelled as shell elements with nonlinear layers. The dynamic properties of the structure, as modes and frequencies, are obtained from the ambient vibrations with Operational Modal Analysis, and for the 3D FE Model by applying the Rayleigh-Ritz method. Time history analysis of known strong ground motions are performed to investigate the response of the 3D FE Model, and study the capturing of the diaphragm effect. Finally, a comprehensive study comparing the captured diaphragm effect with the level of detailing of the diaphragms in the 3D FE model are performed.

The investigated building

The building selected for this study is The City Crest Tower in downtown Vancouver, Canada, the building is a high-rise with flat slab and edge columns with one concrete core and very limit shear walls. The low shear wall ratio enhance the possibility to investigate the diaphragm movement, and avoid the measurement being biased from shear walls. It is of interested to investigate this type of buildings, because the real repose of the diaphragm is simply not known. The diaphragm is often simplified to be a rigid element, but the engineers are missing research where experimental and numerical result are compared to validate this assumption.

The City Crest Tower is a 32-storey podium tower with multiple irregularities and especially the setback at level 10. The floor plan of the tower is non-symmetry, and the outer dimensions for a general floor are 28 m x 24.7 m, see Figure 1. At the second floor, the floor is extended with a 10.8 m x 18 m terrace, which is of special interested for this study. The instrumentation of the building was performed in the summer of 1993, for the terrace setup four sensors were place along a line in the middle of the diaphragm, and the sensor's measurement direction is orthogonal to the sensor line.

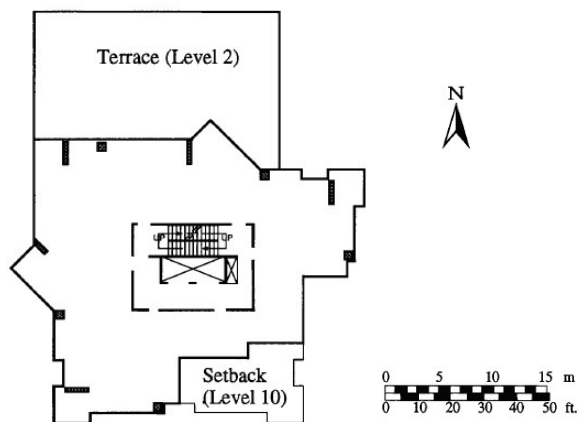


Figure 1, left: floor plan of the City Crest Tower.

Performance of the research

Through ambient vibrations and performing Operational Modal Analysis (OMA) the dynamics properties for both the diaphragm and the global structure are determined. The methods used to determine the frequencies and damping are Enhanced Frequency-Domain Decomposition (EFFD) and a Stochastic Subspace Identification (SSI) in the software program ARTEMIS Modal Pro. In order to isolate the dynamic modelling of the diaphragm and the global structure, the 3D FE Model is a twostep procedure.

First, the diaphragm is modelled and the dynamic properties are determined with Rayleigh-Ritz method. The diaphragm model is updated to match the OMA results, by changing different parameters of the diaphragm. The Modal Assurance Criterion is a key method to match the modes from the real response and the FE Model.

The second step is to model the global structure with the updated diaphragm model. When updating the global model to match the OMA results, the diaphragm will not be changed. This way it's possible to exam the diaphragm and the global structure as two isolated problems.

A comprehensive 3D FE Model, is not always perform when designing these structures, thus this research will look into how detailed should engineers model the diaphragms, to capture a satisfying behaviour. The diaphragm will be model in different detailed levels, and through a time history analysis of different strong ground motions, the responses from the different diaphragm models are investigated.

OMA results

The results from the Operational Modal Analysis shows the first modes in NS and EW are closed spaced at 0.57 Hz and 0.64 Hz with a damping of 2.88 % and 3.41 % respectively. Frist torsional mode at 1.26 Hz with 2.31% damping. The damping ratios corresponds to the recommended literature values of 3-5 %, for reinforced concrete structure with working stress. Figure 2, illustrates the modes from the OMA, 14 modes are determined, the modes in the range of 0-10.5 Hz are associated with the entire structure, and the two modes above this range are associated to the diaphragm of the second floor.

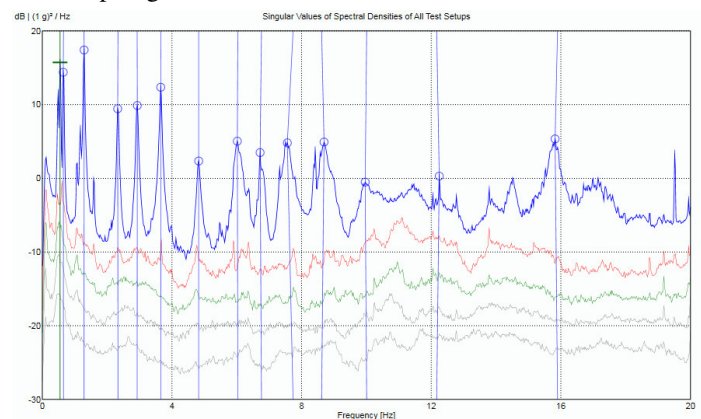


Figure 2, Singular Values of Spectral Densities.

Future

The future phase of this research project is to start the modelling phase in a FEM program and step into the modeling updating part.